

Optical Characterization of the Air-Sea Interface

Erik J. Bock and Wade R. McGillis

Department of Applied Ocean Physics and Engineering
Woods Hole Oceanographic Institution
Woods Hole, MA 02543 USA

Abstract—Optical techniques to measure short wave structure have been developed into working in situ devices in recent years. These devices generally fall into two categories, one category contains devices that make instantaneous 'maps' of surface slope in two dimensional space, and the other category makes time and space series of surface slope at a single point. This paper describes results obtained with a device from the latter category. Data analysis is performed to compute an estimate of surface curvature and it is compared to a short-time scale measurement of wind speed and microlayer chemical enrichment.

I. INTRODUCTION

For long gravity waves, wave energy is inferred from wave height. For capillary waves, wave energy is inferred from wave curvature. This is because for any instant in time the potential energy is given as:

$$E = \rho gh + C\sigma \quad (1)$$

where E is the local potential energy, ρ is the water density, g is the gravitational constant, h is the local wave height, σ is the surface tension, and C is the local curvature.

Information about short wave propagation on the ocean is important since it is the short waves that are the scattering elements responsible for radar backscatter, and radar remote sensing is fundamental to meso- and large- scale monitoring of the ocean surface. Data products of radar remote sensing are useful not only for tactical defense problems, but also for incorporating wind speed estimates into predictive weather models and climate studies. Because short waves are also strongly influenced by the presence of surfactants, remote sensing has been used in the study of oil-spill containment and naturally occurring surfactants produced biologically. Recent studies have indicated a strong correlation between wave slope and gas transfer rates in laboratory and field studies implying that remote sensing of small scale slope or curvature can be useful in estimating gas transfer rates and fluxes. Because the energetics of short waves are strongly represented in curvature, it is this quantity we wish to study.

The results presented in this paper were obtained during the Coastal Ocean Processes - Marine Boundary Layer experiment

This work was sponsored by the National Science Foundation under research grant OCE9410537. This is WHOI contribution number 9332.

off the California coast in April and May of 1995. The experiment included meteorological characterization of the wind forcing of surface waves and turbulence as well as physical and chemical characterization of the air-sea interface.

II. EXPERIMENTAL TECHNIQUES

A. Wind Speed

Wind speed was measured at a height of 10 m using a sonic anemometer fixed to the top of a bow-mounted mast on the Research Vessel *New Horizon*. The anemometer was sampled at 100 Hz, subaveraged, and stored at 25 Hz. During the course of the experiment the ship was pointed into the wind to within 10 degrees so as to avoid flow distortion.

B. Surface Curvature

Computation of surface curvature is defined within the context of this paper as the component of surface curvature tangent to a scanned circle, computed from two successive measurements of surface slope taken at essentially an instant in time (16 μ s apart).

A scanning laser slope gauge [5] has been developed at Woods Hole Oceanographic Institution for the purpose of making measurements of short capillary and capillary-gravity wave spectra in conjunction with radar remote sensing. During the spring experiment, the scanning laser slope gauge was deployed from the Ladas research catamaran. Ladas is a 4.9 m aluminum catamaran that exhibits well-controlled towing and driving capabilities in addition to accommodating a research payload of about 500 kg. The slope gauge on Ladas uses the refraction of a narrow beam (order 0.001 m) by the local slope of the air-sea interface. The scanning system uses a digitally controlled synchronous motor to accurately scan a circle of diameter equal to 0.15 m. At 150 points around the perimeter of this circle, the two components of surface slope η_x and η_y are measured. Their combination results in a slope vector that can point in any arbitrary direction. These measurements are recorded periodically at a rate of 104.17 Hz and stored digitally. Fig. 1 depicts a scan and two representative slope vectors taken at θ_i and the next consecutive point, θ_{i+1} . An enlarged view of these vectors is shown in Fig. 2. Here the two slope vectors are projected onto s , the tangent of the scan circle. The difference between the projections, divided by the distance between the two points ($\delta=0.00314$ m) yields the curvature in the direction

of $\pi-\theta$ as:

$$C_{\pi-\theta_i} = \nabla_s \cdot \nabla \eta_{\theta_i} \quad (2)$$

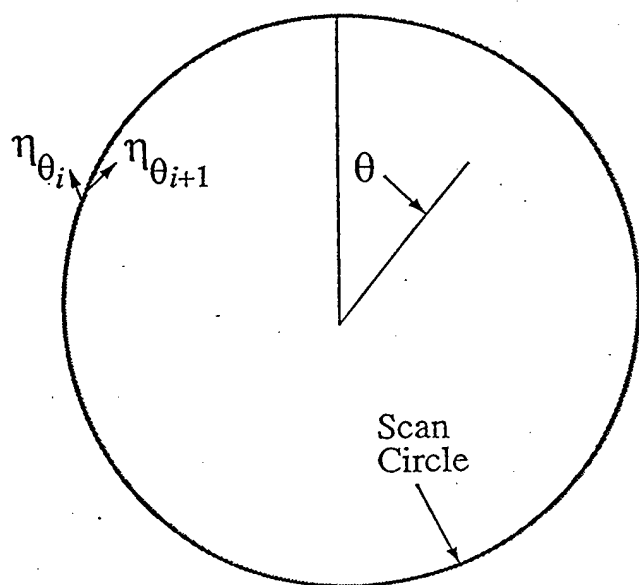


Fig. 1. Scan circle used in the scanning laser slope gauge during the spring experiment off California. Scan circle diameter is 0.15 m. Slope measurements were obtained for θ between 0 and 2π . Representative slope vectors for consecutive samples are shown for arbitrary θ_i .

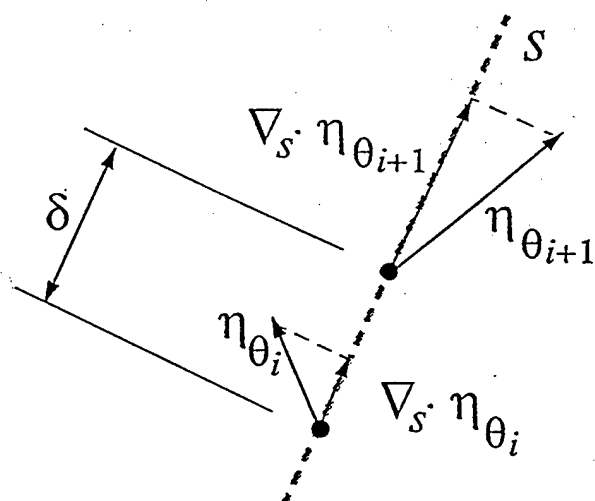


Fig. 2. Expanded view of the sequential slope vector measurements along the tangent of the scan circle, s . Directional curvature is computed using differences in the projected slope components and the distance δ according to (2).

Owing to the symmetry of the scanning pattern, this calculation allows a direct estimate of directional curvature. Rectilinear scanning patterns do not lend themselves as readily to such equal statistics because only in the limit of continuum sampling does the rectilinear pattern allow any arbitrary direction with the same distance, δ , between two points. If different distances between points are used for different directions, the curvature being computed by slope differences is being computed on varying spatial scales. In fact, if large distances are required for arbitrary directional resolution, the definition of curvature based on finite differences of slope breaks down since shorter waves will become aliased. Our current technique, with its associated $\delta=0.00314$ m aliases all waves with wavenumbers higher than about $k=500$ rad/m.

C. Microlayer Colored Dissolved Organic Matter

Surface chemical concentrations were assessed using a surface microlayer sampler. The sampler, deployed directly behind the slope gauge on Ladas, used a rotating glass drum to continuously skim the upper 40-80 microns of the sea surface. A fluorometry package measured the fluorescence emission of the colored dissolved organic matter (CDOM) in the sampler flow stream at 450 nm (excitation at 350 nm). Fluorescence of a second flow stream from 10 cm depth was also measured to provide a measure of bulk seawater CDOM concentration and, thus, the surface microlayer enrichment.

The raw microlayer fluorescence data from the experiment have been calibrated with quinine sulfate standards and normalized to the water Raman band to provide normalized fluorescence. Considerable variability in both microlayer and bulk fluorescence was observed during individual tows as the ship crossed current boundaries. However, additional variability in microlayer fluorescence was attributable to surface chemical features where surface active organic matter was enriched relative to bulk levels. These features, with spatial scales on the order of 10-500 m coincided with reductions in short wave amplitude. Surface chemical features were most prominent at low to moderate wind speeds 1-5 m/s, and tended to erode rapidly with increasing wind stress. However, small microlayer CDOM was detectable at higher wind levels.

III. RESULTS AND DISCUSSION

A. Atmospheric Forcing

Fig. 3 shows a three panel plot of wind speed, omnidirectional surface curvature, and microlayer CDOM for a three hour transect on JD135. Wind speed was used because it could be measured on much shorter time scales than would be required for estimates of wind stress. The importance of a fast response stems from the fact that short capillary waves have very short growth and decay times and that surface curvature is also a very

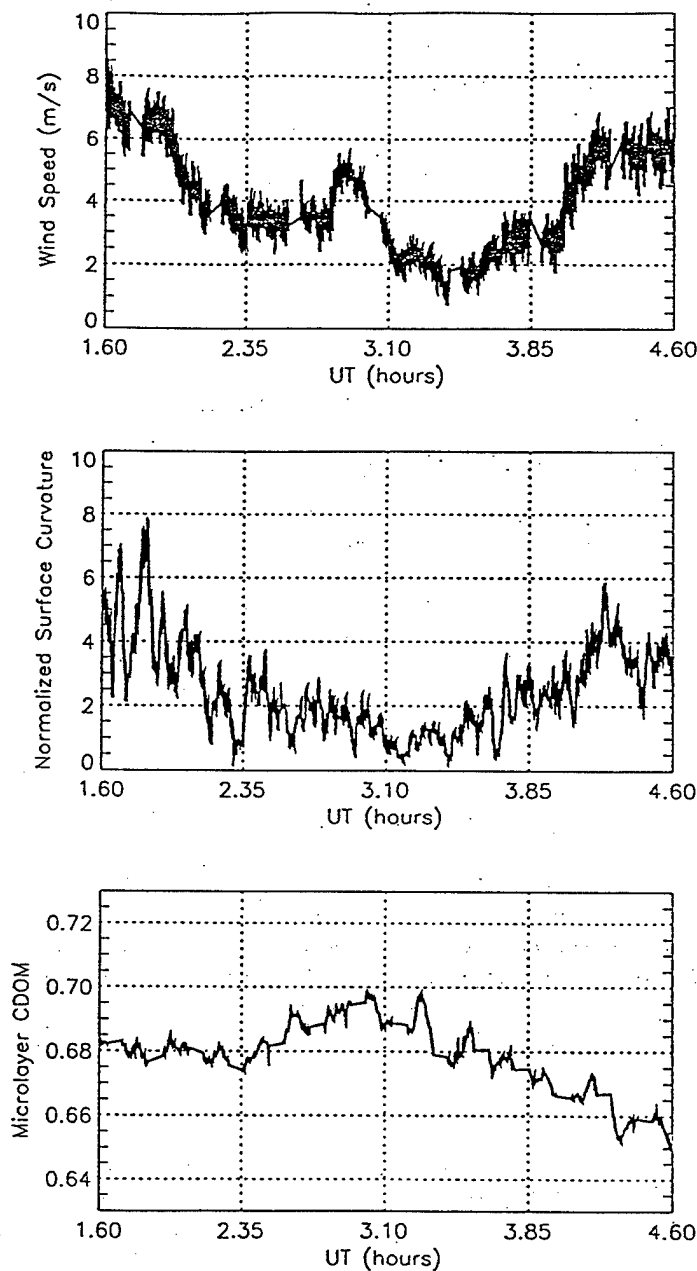


Fig. 3. Three panel plot of wind speed, omnidirectional surface curvature, and microlayer CDOM for a three hour time period on Julian Day 135 during the CoOP-MBL experiment off the coast of California. Time is expressed in fractional hour of the Julian Day. General agreement between wind speed and curvature is observed, even on short time scales. Clear disagreement occurring near 3.0 UT may be explained by elevated levels of microlayer CDOM.

rapidly varying statistical quantity from which to infer estimates of short wave energetics. The omnidirectional surface curvature was computed by integrating the magnitude of the directional curvature for a period of one second and is defined by:

$$\bar{C} = \sum_{\theta=0}^{208\pi} |C_{\theta}| \quad (3)$$

This quantity is computed from 104 scans. Each scan includes 150 directions of curvature. While this provides many directional estimates of curvature, the angular resolution is impaired by the cosine-tapered window that is applied as a result of the projection scheme described by (2). Nevertheless, the high rate of acquisition and the large number of directional vectors used in this technique allow direct comparison between

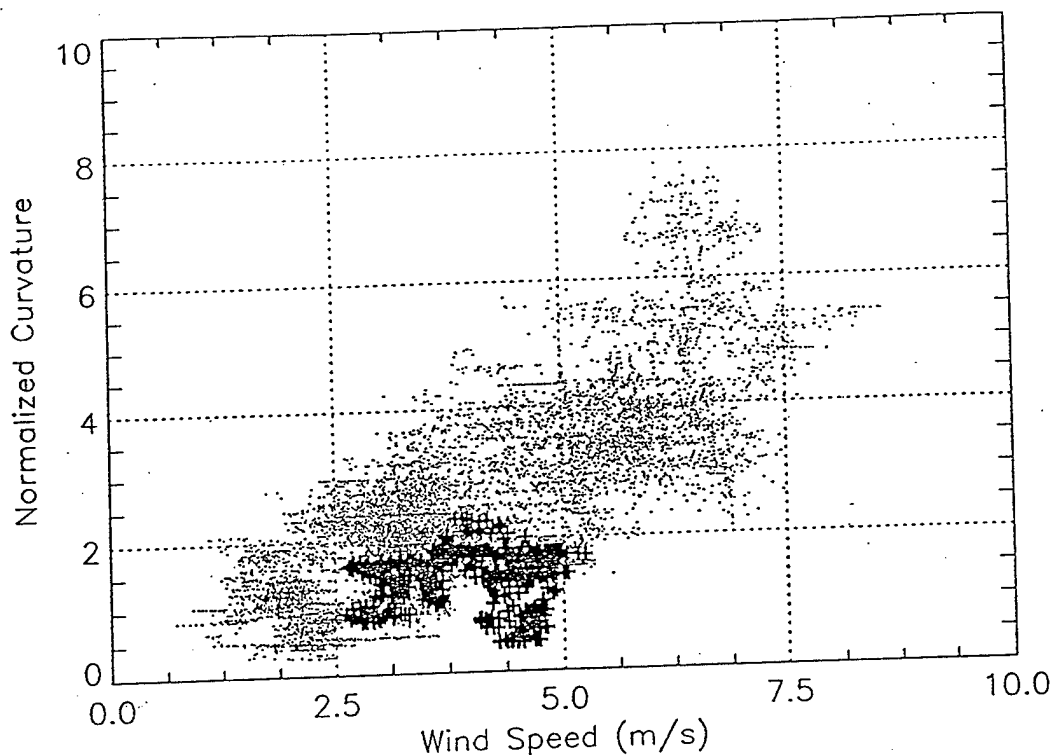


Fig. 4. Scatter plot of the time series presented in Fig. 3. A systematic relation between wind speed and surface curvature is evident from the single points (•) that represent all the data in Fig. 3 except for those between 2.9-3.1 UT. Plus symbols (+) represent data points within the period 2.9-3.1 UT, during which elevated levels of microlayer CDOM were observed.

the top two panels. The general agreement between wind speed and curvature supports the conclusion that curvature can fluctuate rapidly in both space and time scales. Some of this fluctuation is clearly due to gustiness or very rapid changes in wind resulting in events like 'cat's paws'. Fig. 4 shows the relationship between curvature and wind speed for all points in the time series.

B. Forcing from Surface Chemical Composition

Some of the fluctuations observed in the curvature data appear uncorrelated with the wind record. As shown in Fig. 3 for times near 3.0 UT, the wind speed is briefly elevated with no concurrent elevation in curvature. It is interesting to note that the microlayer CDOM levels peak at this time. A possible explanation for the discrepancy between wind speed and curvature is the result of elevated surfactant levels with possible enhanced wave damping. Evidence for this hypothesis is given in Fig. 4. Most of the points represent one to one correspondence between the two parameters. For the interval between 2.9 to 3.1 UT, the data is shown as plus symbols. During this interval, the moderate wind speeds correspond to a curvature which is consistently lower than the mean curvature. This implies that surface curvature can be strongly modulated by the surface composition of surfactants.

If the points depicted as plus symbols are omitted from the scatter plot in Fig. 4, a new scatter plot results. This is shown as Fig. 5. Omission of the data points suspected to be affected most by the presence of surfactants collapses the scatter significantly. The line included in Fig. 5 should not be interpreted as a parameterization since the absolute values of surface curvature are not provided. Rather it should be used as a qualitative indication for assessing the distribution of points about their fit.

IV. CONCLUSIONS

Directional curvature can be readily computed from a circular scanning pattern with a scanning laser slope gauge. Although the technique makes use of only one component of the spatial derivative of slope, enough statistical information is retained to allow fast time response estimates of curvature, and hence, short wave statistics. This information allows fast time comparison with other physical and chemical measurements of the air-sea interface. In situ curvature measurements were obtained with concomitant measurements of both wind speed and surface chemical concentration of CDOM. Clear evidence for a functional relation between surface curvature and these parameters was demonstrated.

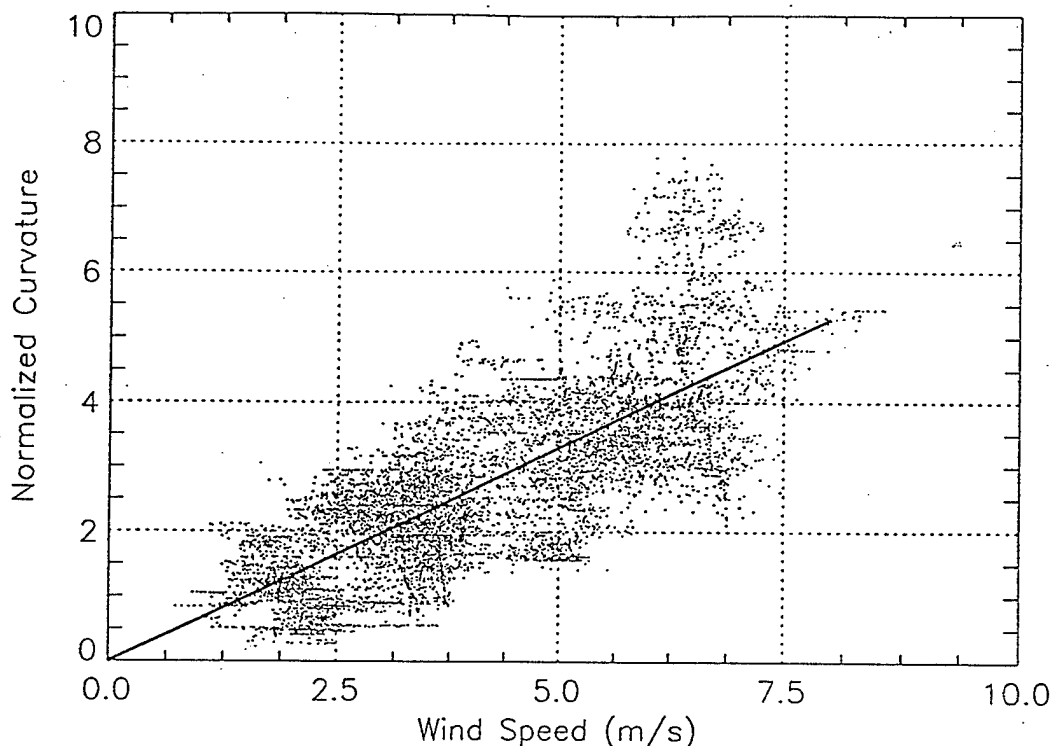


Fig. 5. Scatter plot of the time series presented in Fig. 3 with the omission of data points in the period between 2.9-3.1 UT. A systematic relation between wind speed and surface curvature is evident from the data, and the scatter has been collapsed in comparison with Fig. 4. The line included in Fig. 5 should not be interpreted as a parameterization since the absolute values of surface curvature are not provided. Rather it should be used as a qualitative indication for assessing the distribution of points about their fit.

ACKNOWLEDGMENTS

The authors should like to thank Dr. Nelson M. Frew for the microlayer colored dissolved organic matter data and Dr. James B. Edson for help with the wind speed measurements and the use of the sonic anemometer.

REFERENCES

- [1] C. S. Palm, R. C. Anderson, and A. M. Reece, "Laser probe for measuring 2-D wave slope spectra of ocean capillary waves," *Appl. Opt.*, 16, pp. 1074-1081, 1977.
- [2] P. H. Lee, J. D. Barter, K. L. Beach, C. L. Hindman, B. M. Lake, H. Rungaldier, J. C. Shatzman, J. C. Shelton, R. N. Wagner, A. B. William, R. Yee, and H. C. Yuen, "Recent advances in ocean surface characterization by a scanning laser slope gauge," *Proc. Optics of the Air-Sea Interface: Theory and Measurements, SPIE*, 1749, pp. 234-244, 1992.
- [3] B. Jaehne and K. S. Riemer, "Two-dimensional wavenumber spectra of small scale water surface wavers," *J. Geophys. Res.*, 95, pp. 11531-11546, 1990.
- [4] P. A. Hwang, S. Atakturk, M. A. Sletten, and D. B. Trizna, "A study of the wavenumber spectra of short water waves in the ocean," *J. Phys. Ocean.*, 26, pp. 1266-1285, 1996.
- [5] E. J. Bock and T. Hara, "Optical measurements of capillary-gravity wave spectra using a scanning laser slope gauge," *J. Atmos. Ocean. Tech.*, 12, pp. 395-403, 1995.